GOME-2 optical degradation as seen in level 2 data time series (2007 – 2010; BrO, NO_2, HCHO, H_2O, and O_3)

Sebastian Dikty[(1)], Andreas Richter[(1)], Mark Weber[(1)], Stefan Noël[(1)], Folkard Wittrock[(1)], Heinrich Bovensmann[(1)], Rosemary Munro[(2)], Rüdiger Lang[(2)], and John P. Burrows[(1)]

(1) Institute of Environmental Physics, University of Bremen, Germany, (2) Eumetsat, Darmstadt, Germany

Contact: Sebastian Dikty, dikty@iup.physik.uni-bremen.de

Universität Bremen

Institute of Environmental Physics

Introduction

The overall aim of the study is to provide input on the following questions:

- What is the effect of GOME-2 degradation on the accuracy (absolute values) of level 2 products?
- What is the effect of GOME-2 degradation on the precision (scatter) of level 2 products?
- Is the degradation dominated by throughput loss or are there also systematic spectral structures linked to instrument changes or degradation related calibration deficiencies?
- Are there possibilities to correct for degradation effects on GOME-2 level 2 products?
- What happened with GOME-2 level 2 products during the throughput test (Sep 2009), and what can we learn from these results?

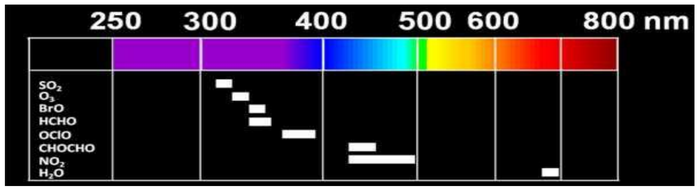

Fig. 2: Fit windows for the retrieval of trace gases from GOME-2 measurements.

GOME-2 vs. SCIAMACHY

In order to assess the magnitude of degradation in vertical columns, RMS, and χ^2 we compare GOME-2 time series from 2007-2010 with the respective time series from SCIAMACHY. In addition, SCIAMACHY time series from 2003-2006 were used to assess the degradation within the first four years of operation. Results can be seen in Figs. 3-7 for HCHO, BrO, NO_2, O_3, and H_2O, respectively. Due to differences in the level 2 output for O_3 and H_2O fit window intensities as shown for HCHO, BrO, and NO_2 could not be retrieved. All time series are based upon monthly means of all values for the given box of geolocations. Results for the Sahara and the Pacific boxes are shown in the upper panels and for the Greenland and Antarctica boxes in the lower panels, respectively.

Selected references

Begoin, M., Richter, A., Kaleschke, L., Tian-Kunze, X., Stohl, A., Burrows, J.P., Satellite observations of long range transport of a large BrO cloud in the Arctic, *accepted for publication in ACPD*, 2009

Noël, S., S. Mieruch, H. Bovensmann and J. P. Burrows, Preliminary results of GOME-2 water vapour retrievals and first applications in polar regions, *Atmos. Chem. Phys.*, 8, 1519-1529, 2008

Richter, A., Begoin, M., Hilboll, A., Burrows, J. P., Improvements in GOME-2 retrievals of NO2, *Proceedings of the 2nd EPS/Metop RAO Workshop*, Barcelona, 2009

Vrekoussis, M., Wittrock, F., Richter, A., Burrows, J. P., GOME-2 observations of oxygenated VOCs: What can we learn from the ratio CHOCHO to HCHO on a global scale, *to be submitted to GRL*, 2009

Weber, M., L.N. Lamsal, and J.P. Burrows, Improved SCIAMACHY WFDOAS total ozone retrieval: Steps towards homogenising long-term total ozone datasets from GOME, SCIAMACHY, and GOME2, *Proc. 'Envisat Symposium 2007', Montreux, Switzerland, 23-27 April 2007, ESA SP-636*, July 2007

Tab. 1: χ^2 as computed for the respective trace gas in GOME-2 level 2 products.

trace gas	shown as
BrO, NO_2, and HCHO	$\chi^2 = \frac{1}{n-1}\sum_{i=1}^{n}(X_i - \mu_i)^2$
O_3	$\chi^2 = \frac{1}{n}\sum_{i=1}^{n}(X_i - \mu_i)^2$
H_2O	$\chi^2 = \frac{cov(p_k, p_k)}{n_d - n_p}\sum_{i=1}^{n}(X_i - \mu_i)^2$

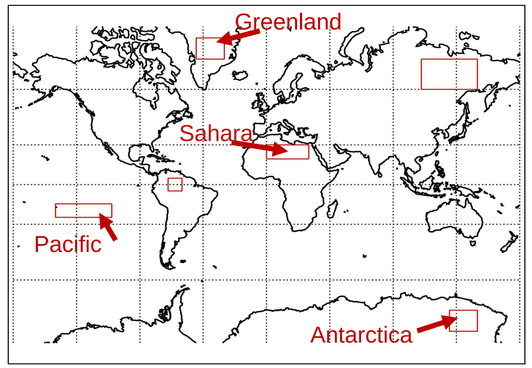

Fig. 1: Boxes of geolocations used to investigate degradation in level 2 data. Three different surface groups have been chosen: Open ocean (Pacific, 25°S-15°S, 150°W-110°W), desert (Sahara, 20°N-30°N, 0°E-30°E), and ice & snow (Greenland, 70°N-75°N, 50°W-30°W and Antarctica, 70°S-75°S, 130°E-150°E). Boxes over boreal- and rainforest (Siberia and Amazon) have been discarded due to high fluctuations (anthropogenic and natural).

GOME-2

spectral range	312 – 800 nm
orbit	sun-synchronous, 820 km
viewing geometry	nadir
pixel size	80 x 40 km²
data available	Jan 2007 - today

Image of MetOp-A courtesy of Eumetsat.

HCHO

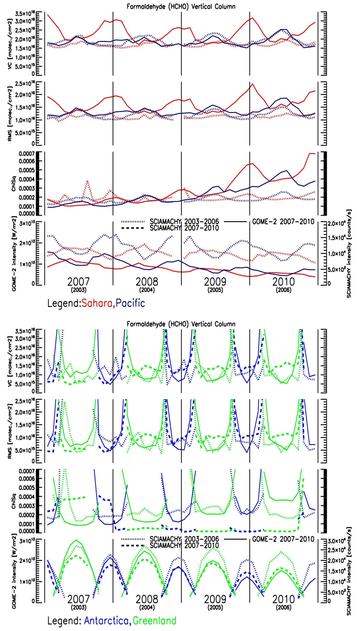

Fig. 3 (above): Time series (2007-2010) of monthly means of GOME-2 HCHO vertical columns over Sahara (red), Pacific (dark blue), Greenland (green), and Antarctica (light blue). Also shown are time series for RMS, χ^2, and intensity. RMS is calculated as the standard deviation of all data within the given box of geolocation (precision). χ^2 resembles the accuracy of measurements. As can be seen, the intensity decreases over the years which is due to the loss of throughput. SCIAMACHY data is plotted in dashed (2007-2010) and dotted lines (2003-2006).

BrO

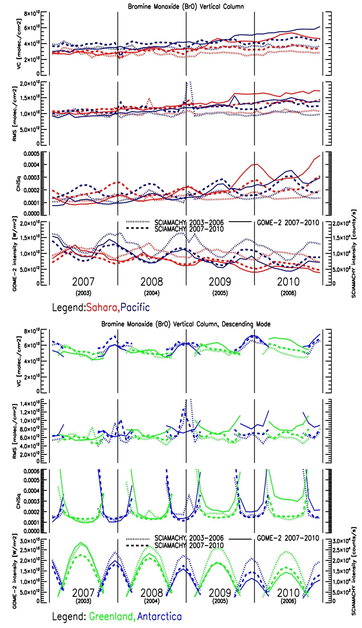

Fig. 4 (above): Same as Fig. 3, but for BrO.

NO_2

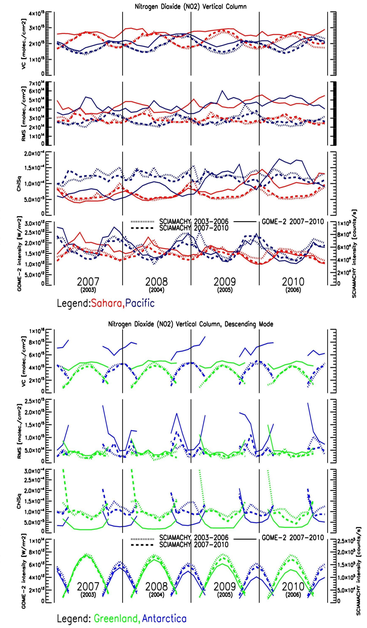

Fig. 5 (above): Same as Fig. 3, but for NO_2.

O_3

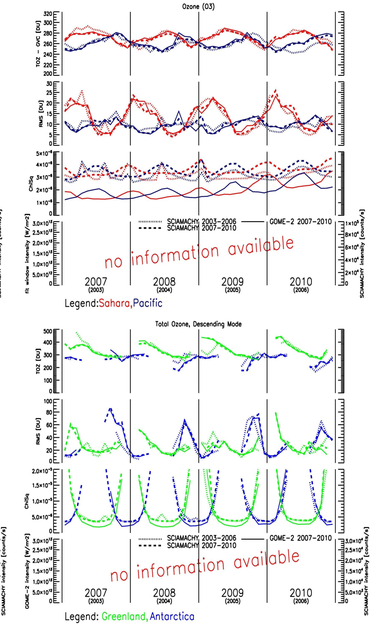

Fig. 6 (above): Same as Fig. 3, but for O_3.

H_2O

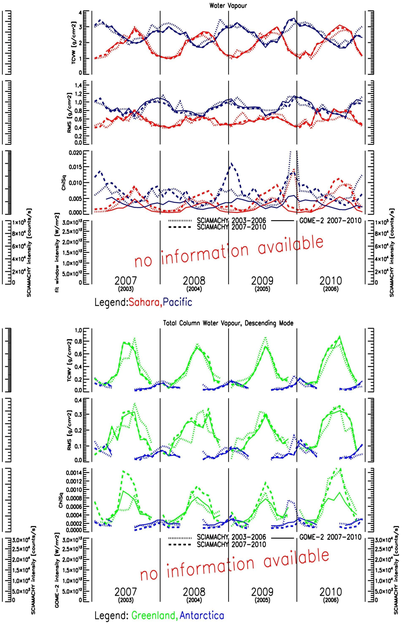

Fig. 7 (above): Same as Fig. 3, but for H_2O.

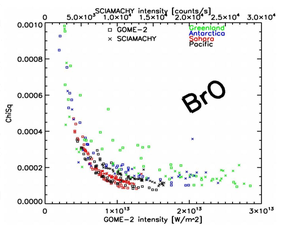

Fig. 8: Intensity dependent retrieval residuals χ^2 for BrO (left) and NO_2 (right). Abnormally increased χ^2 from GOME-2 BrO over Greenland in 2010 can be seen as also visible in Fig. 4. SCIAMACHY NO_2 χ^2 have a systematic disagreement to the $1/(INT)^2$ dependency.

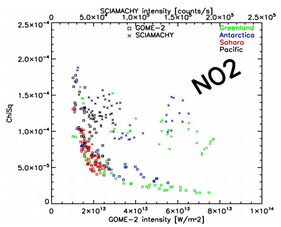

Summary

In general, the signs of degradation are less obvious for strong absorbers in the visible close to the infrared, like H_2O. Although fit residuals (χ^2) strongly increase for O_3, vertical columns are not effected. Unlike for BrO and HCHO, where fit residuals highly increase and an effect in the vertical columns is visible.

Acknowledgements: We thank Eumetsat for providing funds and the SCIAMACHY science team at IUP Bremen for providing SCIAMACHY data sets for comparisons with GOME-2.